The EUMETSAT Network of Satellite Application Facilities

ROM SAF

Radio Occultation Meteorology

EUMETSAT Satellite Application Facility on RO Meteorology

CDOP-2 Visiting Scientist Report 17:

Analysis of GRAS interference patterns

Oscar Isoz

Danish Meteorological Institute (DMI)
European Centre for Medium-Range Weather Forecasts (ECMWF)
Institut d'Estudis Espacials de Catalunya (IEEC)
Met Office (MetO)

Ref:
SAF/ROM/DMI/REP/VS17/001
Version: Version 1.0
Date: 16 Sept 2012

DOCUMENT AUTHOR TABLE

	Authors(s)	*Function*	*Date*	*Comment*
Prepared by:	Oscar Isoz	ROM SAF Visiting Scientist	10/09/12	
Reviewed by:				
Approved by:	Kent	ROMSAF	16/09/12	

DOCUMENT CHANGE RECORD

Issue/Revision	*Date*	*By*	*Description*
Version 1.0	16 Sept 2012	Oscar Isoz	

VS Authors

This VS study was carried out by Licentiate Oscar Isoz, LTU Kiruna, Sweden; Email: oscar.isoz@ltu.se.
(In Sweden, a 'Licentiate' is an intermediate degree between MS and PhD, usually after two years of PhD studies.)

VS Duration

The VS study was performed during May-June 2012 and included a one week visit in May 2012 to EUMETSAT, Darmstadt, Germany and a three weeks stay in June 2012 at the Danish Meteorological Institute, Copenhagen, Denmark.

List of Contents

Executive Summary

The main objective of this VS was to analyze interference patterns in the GRAS data.

By analyzing recorded raw sampling data from Oct 2007, it was possible to estimate that about 50% of the received occultations contained only the tracked occulting GPS satellite and less than 4% contained pulsed interference. The rest of the analyzed occultations contained either multiple signals or had too little raw data to be analyzed. It will be shown that the pulsed interference was mainly received when GRAS recorded occultations in the northern Pacific. To determine if interference had any significant impact on the quality of the bending angle, pre-calculated (O-B)/B were used and then an (O-B)/B histograms was made for clean occultations, occultations with pulsed interference and then occultations with multiple signals. There were no significant difference between the three histograms.

1. Introduction

1.1 Purpose of Document

This document presents the results from EUMESAT ROMSAF VS 17 that was performed during the summer of 2012. The objective of the VS was to analyze interference patterns in GRAS data and to determine if interference has any impact on the quality of the RO measurements.

1.2 Applicable & Reference documents

Reference Documents

[RD.1] Bastide, F., Akos, D., Macabiau, C., and Roturier, B., Automatic gain control (AGC) as an interference assessment tool, in *ION GPS/GNSS 2003*, Institute of Navigation, 2003.

[RD.2] Bonnedal, M., GRAS on MetOp - instrument characteristics and performance evaluation, in *OPAC 2010*, 2010.

[RD.3] ESA, Sea surface salinity SMOS satellite measurements improve as ground radars switch off, 2012.

[RD.4] FAA, Spectrum management regulations and procedures manual, Order 6050.32B, FAA, 2005.

[RD.5] Gibbons, G., Your signal is my noise, raising questions of gnss compatibility and interoperability, *Inside GNSS*, *Jan/Feb*, 2011.

[RD.6] Lampert, T. A. and O'Keefe, S. E. M., A survey of spectrogram track detection algorithms, *Applied Acoustics*, *71*, 87–100, 2010.

[RD.7] Lo, S., Akos, D., Eklöf, F. M., Isoz, O., and Borowski, H., Detecting false signals with automatic gain control, *GPS World*, *April*, 2012.

1.3 Definitions, acronyms and abbreviations

(O-B)/B	A comparison between forecasted and observed bending angle, often used as quality measure.
COSMIC	Constellation Observing System for Meteorology, Ionosphere & Climate
DMI	Danish Meteorological Institute
ECMWF	The European Centre for Medium-Range Weather Forecasts
EPS	EUMETSAT Polar System
ESA	European Space Agency
ESTEC	European Space Research and Technology Centre (ESA)
EU	European Union
EUMETSAT	European Organisation for the Exploitation of Meteorological Satellites
GALILEO	European GNSS constellation project (EU)
GLONASS	Global Navigation Satellite System (Russia)
GNSS	Global Navigation Satellite Systems (generic name for GPS, GLONASS and the future GALILEO)
GPS	Global Positioning System (US)
GRAS	GNSS Receiver for Atmospheric Sounding (onboard Metop)
GRAS SAF	Consortium formed to define and prepare the Operational GRAS SAF. Members are DMI (leader), UKMO and IEEC.
LOS	Line Of Sight
METOP	Meteorological Operational polar satellites (EUMETSAT)
MPEF	Meteorological Products Extraction Facility (EUMETSAT)
N/A	Not Applicable or Not Available
NOAA	National Oceanic and Atmospheric Administration (US)
Operational GRAS SAF	Team responsible for the handling of GRAS data and the delivery of meteorological products during the operational life of the instrument
RO	Radio Occultation
ROC	Radius Of Curvature
ROPP	Radio Occultation Processing Package
SAF	Satellite Application Facility (EUMETSAT)
TBC	To Be Confirmed
TBD	To Be Determined
UTC	Universal Time Coordinated
VS	Visiting Scientist
WGS-84	World Geodetic System, 1984. (US DoD)

2. Background

Any transmission is a potential source of interference for other receivers, or as Glen Gibbons stated it "Your signal is my noise" [RD.5]. But just because a signal can be detected it does not mean that it will cause an issue or measurably degrade the performance of the receiver.

Earlier research has shown that some instruments are fairly sensitive to ground based transmissions, one such instrument is the "Soil Moisture and Ocean Salinity" (SMOS) mission who's data quality improved when a number of ground based transmitters was turned off/moved in frequency [RD.3]. The GRAS receiver tracks signals from GPS satellites that has passed through the atmosphere. Bonnedal et al [RD.2] has shown that other signals than the occulting satellite can be detected in the output from the receiver. One might ask if ground based transmitters can cause a degradation of the data quality or if the receiver will loose tracking of the satellite before there is any impact on the measurements.

GNSS satellites uses a Pseudo Random Number (PRN) code to spread out the satellite power over a wider frequency band and enable multiple satellites to share the same frequency. One limitation with the public GPS Coarse Acquisition (C/A) PRN code is that it has side lobes that are around 25dB weaker then the main peak. When the receiver is tracking a satellite that is attenuate by the atmosphere, then the side lobes of the correlation peak from other satellites can appear in the tracked data.

The GNSS L1/E1 frequency band (centered at 1575.42MHz) is protected so there are not supposed to be any other transmissions besides those from other GNSS satellites on that frequency. The L2 signal is centered around 1227.6MHz and is located in the lower end of a frequency band that is used by ground based air control radars (1215-1400MHz)[RD.4].

3. Detection of Interference

Interference can be detected at various stages in the receiver chain. The later in the receiver chain the detection is done, the more will usually be known about the impact on the receiver, but more information about the interfering signal will be lost. The opposite is also true, the earlier in the receiver chain the interference is detected, the harder it is to predict the impact of the interference on the final measurement.

The first indication that a GNSS receiver is subjected to additional transmitters is measure the power of the received signal.When the GNSS signal reaches the receiver it is weaker than the background noise. This means that if the receiver configuration is constant (as it is for GRAS), the received signal strength will only change significantly if there are additional signals in the GNSS band.

It should be noted that a change in received signal energy does not automatically mean that there will be any change in the performance of the receiver. The idea of using the measured received signal level as a method for interference detection has been explored in a number of papers such as [RD.1] and more recently [RD.7].

The GRAS L0r data files have a variable called "gain signal" that indicates how much gain the GRAS receiver applies to the incoming signal.

The receiver stores information about the de-spreading of the received GPS signal in a number of variables. When the signal is weak the receiver uses an estimated model of how the satellite will move and uses something called "raw-sampling" mode in which it records in-phase and quadrature-phase (IQ) data (and other variables) at a rate of 1kHz. Closed loop mode is used when the received signal is strong enough for the GRAS to use the received signal to steer its internal tracking loops, during closed loop mode the data (such as the IQ data) is only saved at a rate of 50Hz. i

These variables have previously been used to detect other signals in the GRAS data [RD.2], where ground reflections, pulsed interference (most likely radar) and other GPS satellites have been detected.

4. Initial Analysis

Using the "signal_gain" variable for both the closed loop data (L2) and raw sampling mode (C/A). Four plots were made to show how the GRAS receiver saw the noise level at various locations around the earth, as shown in Figure 4.1. Since the plot is based on L0r data, the location of the dots are the satellite positions. Figure 4.1 is a merged plot of data from the first

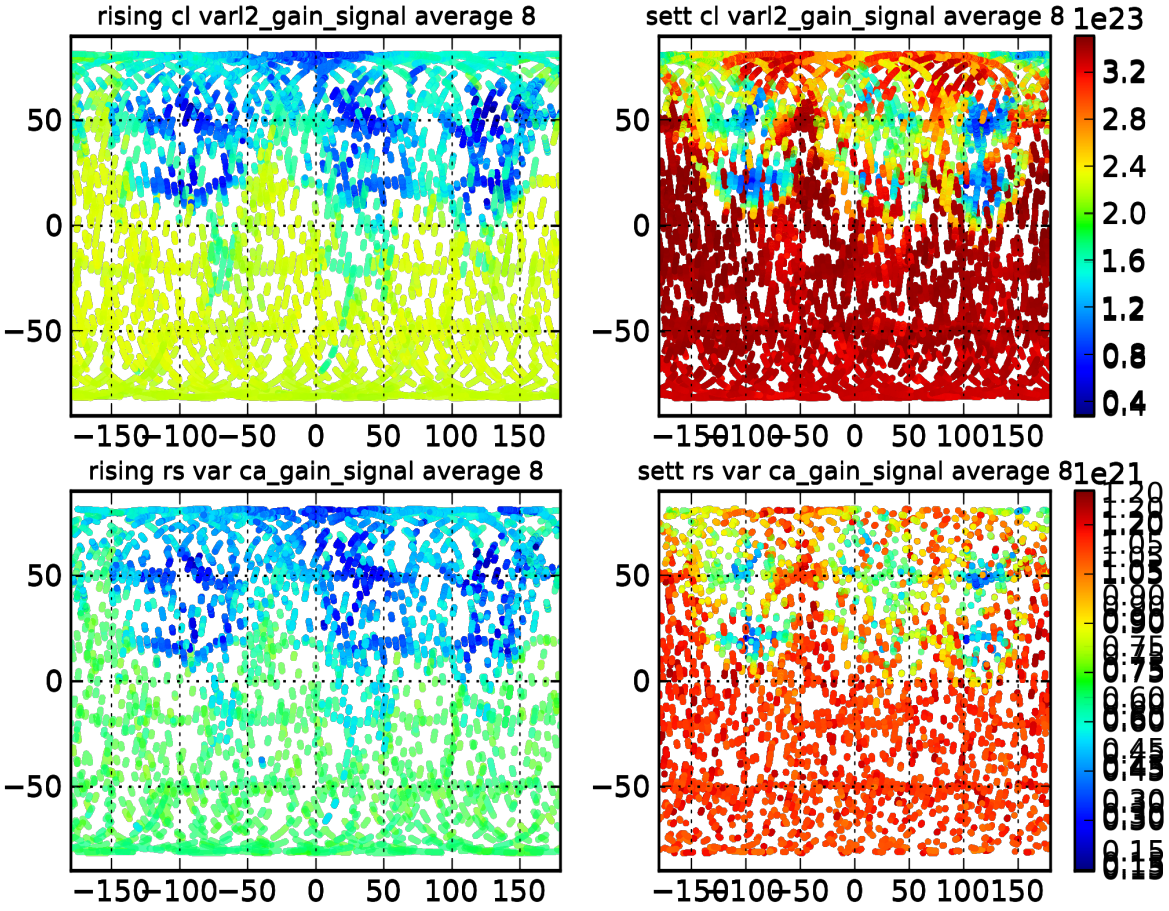

Figure 4.1: Amount of gain applied to the received analog signal by GRAS vs satellite position.

6 days of October 2007, i.e. six separate plots with a transparent background has been on top of each other. To reduce the number of plotted data points each 'dot' shows the average between eight consecutive data points. It shows that that the noise floor varies both with satellite position and the direction of the antenna (e.g. upper right plot at position 50N, 100E). It is plausible (but not verified) that the signal gain measurement would make it possible to detect events such as military GNSS jamming exercises that does not have enough power to affect the performance of the receiver significantly.

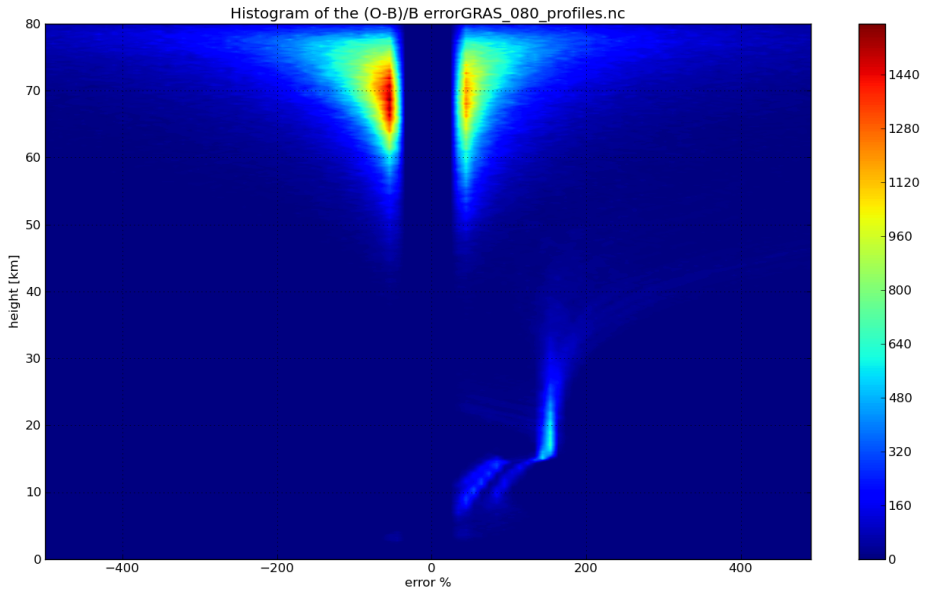

Figure 4.2: histogram over ROPP occultatins with atleast 40% (O-B)/B signal error

One method to determine the accuracy of the retrieved bending angles is to compare them with bending angles from ECMWF and calculate the (O-B)/B value where B is the background ECMWF calculated bending angle and O is the observed RO bending angle. ROMSAF provided pre-calculated (O-B)/B that was used to generate a plot to determine if the histogram could reveal anything.

The plotted values can be seen in Figure 4.2, something seems to happens at about 15km. It was later concluded that the ridge close to +150 percent error was caused by loss of lock on L2 and therefore loss of Ionospheric correction.

4.1 L1b Full Plot

A script was written in order to get an initial overview of how different aspects of the signal affected the resulting bending angle. The script generates a figure that shows a number of variables for a particular occultation based on data from the L1b and the corresponding L0r file. An example of a figure generated by the script can be seen in Figure 4.3. The numbers in the figure are explained in the list below.

1. The name of the file processed.
2. The bending angle (P1, P2 and the modeled).

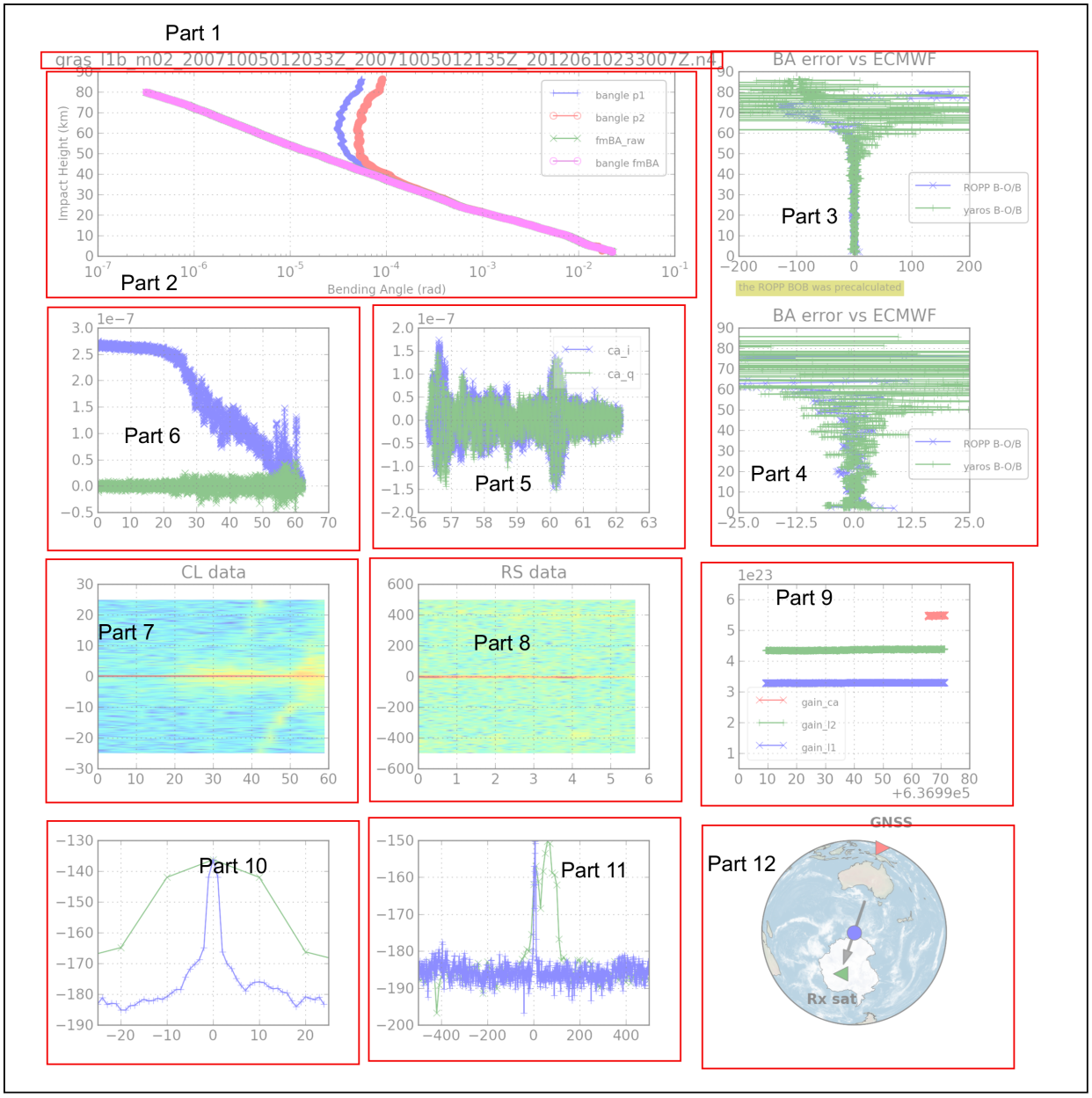

Figure 4.3: RO dataset with parts named

3. The (O-B)/B (where 0 is perfect match between the forecast bending angle and the calculated bending angle. It is used as a standard quality measure in the RO community. It shows the relative difference between an interpolated ECMWF and the interpolated bending angle calculated by the yaros software (green) and the ROMSAF-ROPP software (blue). The ROPP bending angles was pre-calculated.

4. The (O-B)/B error relative an interpolated ECMWF, zoomed to show small errors better.

5. The open loop output from the I and Q data in the time domain.

6. The closed loop output from the I and Q data in the time domain.
7. The spectrogram of the closed loop signal, I+i*Q (sometimes called IQ) data.
8. The spectrogram of the open loop signal, I+i*Q data.
9. The "signal gain" variable - i.e. a measure of how much gain the receiver applies to the received signal.
10. The power spectral density of the open loop data. Green line is a zoomed in version of the blue line.
11. The power spectral density of the closed loop data and the Green line is a zoomed in version of the blue line.
12. The location of the receiver (green triangle), occultation (blue dot) and GPS sat (red triangle).

The initial visual inspection did not reveal any obvious correlation between any parameter and the variations in (O-B)/B error.

4.2 Identified Signal Features

Using the script described in the previous section, three different types of signal features was identified

1. Pulsed transmitters that causes peaks in the spectrogram separated by about 31Hz - (High pulse repetition frequency).
2. Pulsed transmitters that causes peaks in the spectrogram separated by about 214Hz - (Low pulse repetition frequency).
3. Traces of other GPS satellites.

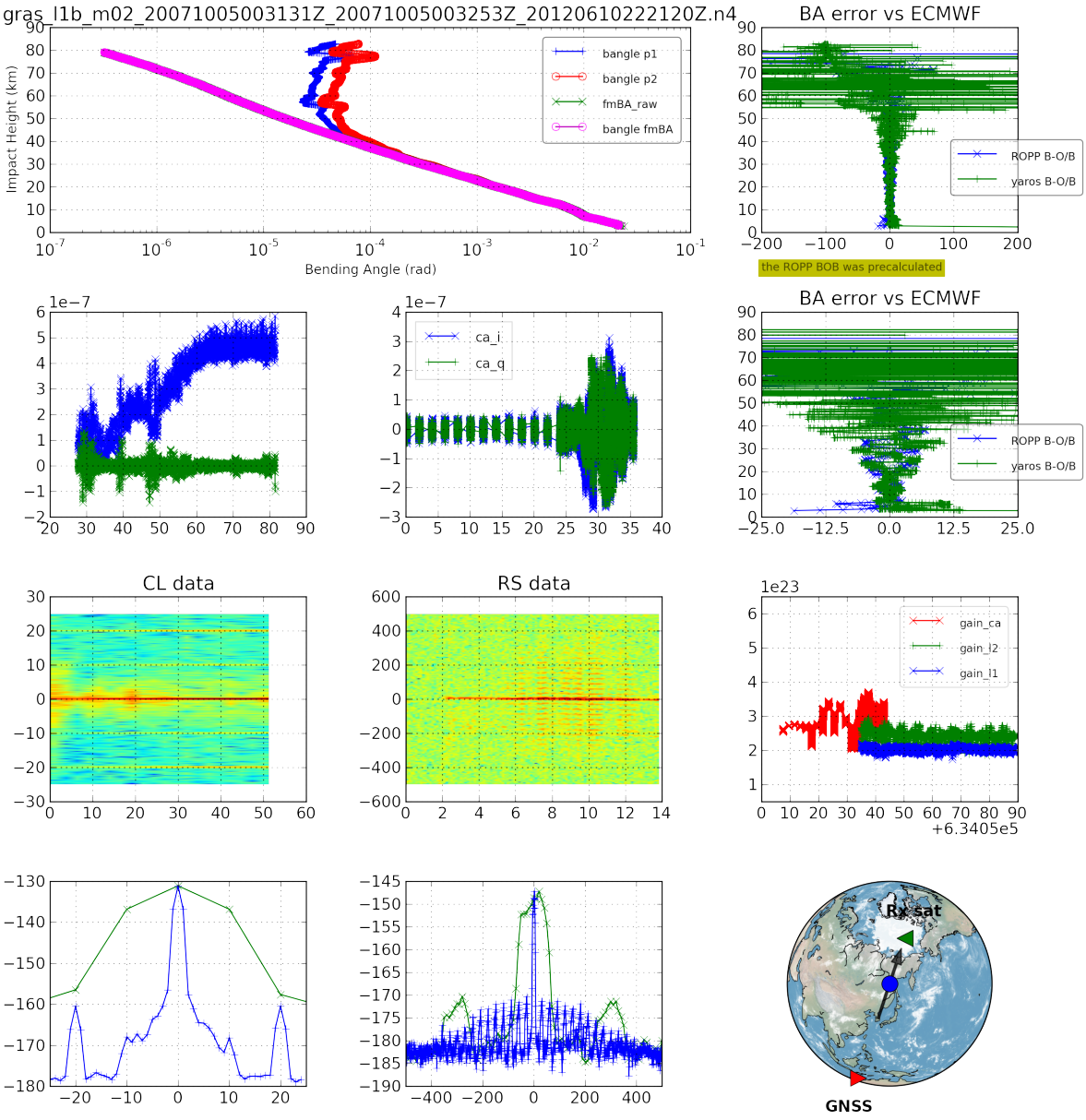

Figure 4.4: Example of a RO dataset with high pulse repetition frequency transmitter

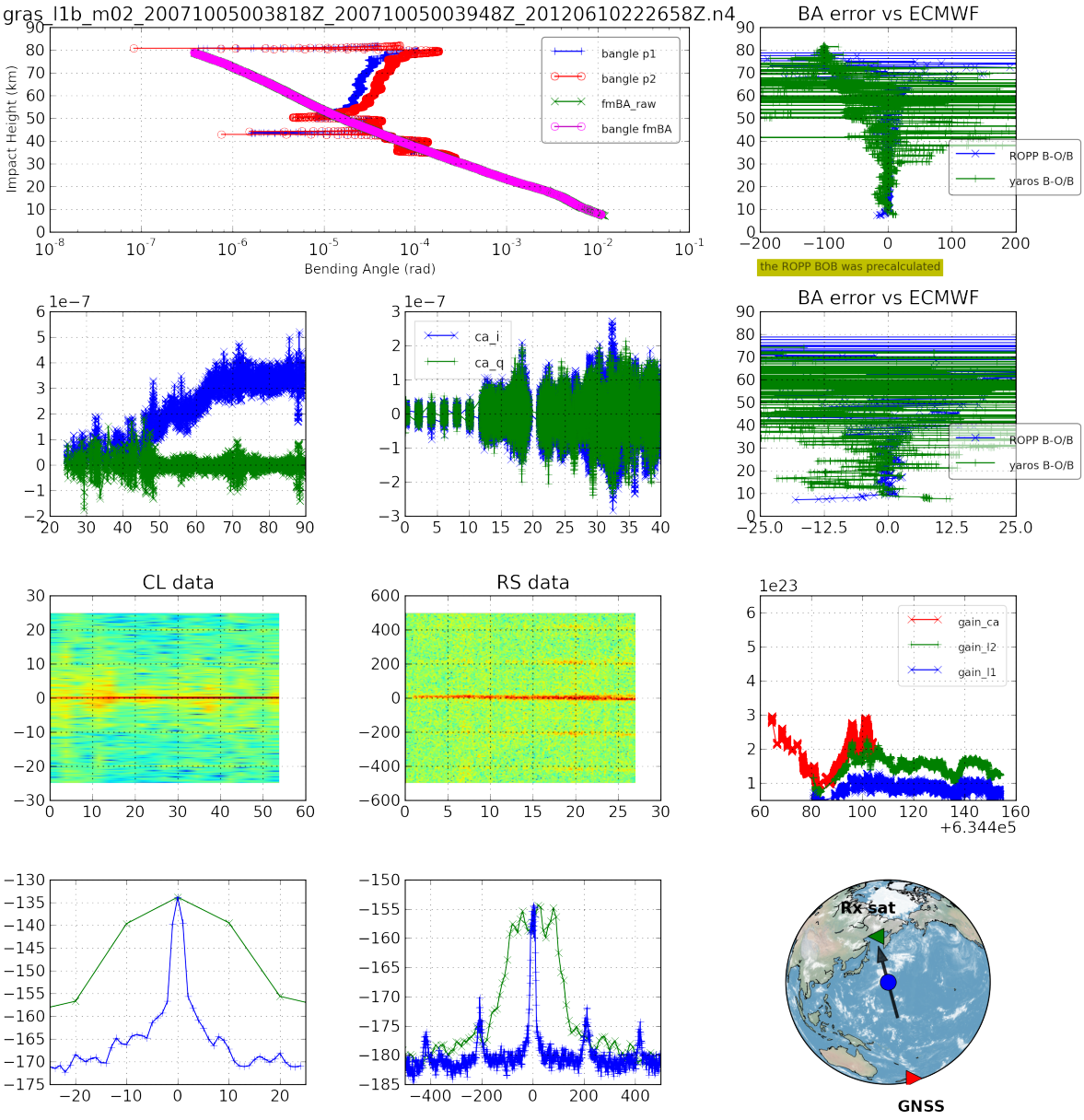

Figure 4.5: Example of a RO dataset with low pulse repetition frequency transmitter

5. Automatic Identification of Features

The initial analysis indicated that no obvious correlation existed between strong received signal power, pulsed interference, other GPS and an increase of the estimated bending angle error. Effort was made to automatically detect various interference sources to determine if anything could be said about the impact based on the statistical errors for occultations with a certain type of interference vs occultations without any interference.

Based on the results of the initial analysis, it was clear that the spectrogram consisted of mainly three different signals:

- the tracked GPS satellite
- other GPS satellites
- pulsed interference (radar)

These three different signals has different appearance in the spectrogram of the raw sampling IQ data. The tracked GPS satellite is usually a track along the centerline, although this might exist or not exist. Due to the limited cross correlation properties of the GPS C/A code, strong GPS satellites can leak into the IQ data and cause straight line tracks in arbitrary directions. Pulsed interference appears as multiple parallel lines, the distance between the lines is dependent on the pulse repetition frequency.

Besides these three features there are also sometimes GPS ground reflections that caused curved lines, no effort was made to detect those.

Due to the properties of the detected signals the identification algorithm should ideally fulfill a number of requirements:

- Detect multiple parallel tracks
- Detect multiple tracks
- Detect crossing tracks
- Detect tracks with an arbitrary starting point
- Detect tracks with an arbitrary end point

In [RD.6] an overview of different methods to process spectrograms is given. Based on that paper it was determined that treating the spectrogram as an image would make the most sense. Treating the spectrogram as an image could also make it possible to reuse/extend the developed method/code for later research where the time-frequency method is changed from the short term Fourier transform to something else. Initially an effort was made to draw lines based on the highest values in the spectrogram. This was made in two ways, first by calculating all possible lines between the peaks and only save the lines with a "good enough" fit. Later the so called Hough transform was also evaluated . Due to lack of progress these two methods were eventually abandoned.

5.1 Proposed Method

The method proposed first low-pass filters the spectrogram before it isolates all areas above a certain threshold. After the areas identified and small areas removed, a least square line is then calculated weighted by the normalized spectrogram power in each point. Radar/pulsed interference is identified by its characteristic appearance in the frequency domain with peaks at a very regular interval. In the table below the method is described in greater detail.

1. Calculate spectrogram (Pxx) with a sampling rate of Fs=1000Hz and 1024bins in the FFT.
2. If max power of the spectrogram is below a certain value, close the file and take the next one.
3. Detect and remove the GNSS peak.
4. Average the spectrogram using a gaussian filer with a kernel of 3x3 pixels.
5. Calculate a binary image where all pixels with a value above mean of the raw spectrogram (Averaged Spectrum) is equal to one else zero.
6. Give each continuous area in the binary image a unique val.
7. Merge areas that are close to each other in time and frequency.
8. For each step in time:
    a) Determine the max, min and position of the peak in each field.
    b) Take the modulus of the frequency difference between the peaks vs the known pulse repetition frequency of the pulsed interference.
    c) If radar is found at more than one time - flag the dataset as interfered by radar.
    d) Remove all areas that contains detected radar interference.
9. Merge areas that are close to each other in time and frequency - larger now after the radar has been removed.

10. Remove all areas that are too small area.

11. Calculated the weighted least square line for all areas. The weight for each point is based the normalized value of the spectrogram.

5.2 Verification

During the development, the algorithm was continuously verified by visually comparing spectrograms with the results of the algorithm. One example of a figure that was used to verify the algorithm can be seen in Figure 5.1. The image has four parts, each showing one aspect of the algorithm.

In the upper left corner the normalized spectrogram is showed after the GPS peak has been removed. The short lines in that figure show the location and size of detected areas with a value above the threshold. In the upper right corner, the spectrogram is seen along the time axis to easily detect radar interference and compare the data with the threshold. If the algorithm detects any other lines than the tracked GPS line, they are shown on the lower left plot. That plot also shows the spectrogram with a value above the threshold, the idea is to easily see if the calculated lines follow the areas with high values in the spectrogram.

Radar detection is not shown in the plots, instead it is written out to the terminal. Finally the lower right plot shows the smoothed spectrogram after the GNSS peak has been removed. When the algorithm became more and more stable the number of datasets used for verification was increased.

Before any extensive analysis were done the algorithm was tested on atleast 200 individual datasets. Particular emphasis was on the accurate detection of the two types of radar signature and that clean datasets had no strong interference. Due to the variation in both, power, length and frequency of the other signals it was determined that accurate calculation of doppler had to be postponed to a later stage.

The verification showed that in many cases both types of radar signature coexisted in the same dataset.

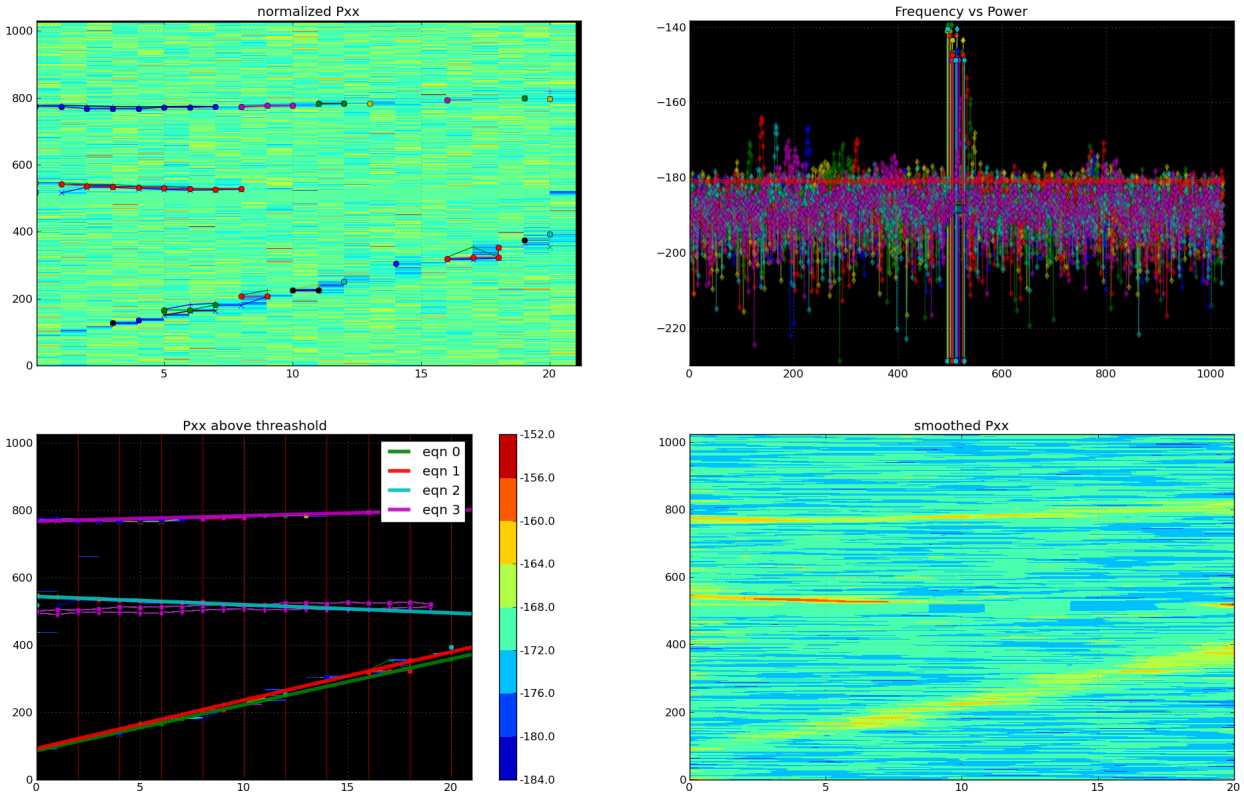

Figure 5.1: four plots used to verify the algorithm

6. Results

The developed algorithm was tested on GRAS L1a data from October 2007 that was processed by EUMETSAT.

6.1 Statistics Over the Number of Occultations with Additional Signals

The data covered was of the type level 1a data and covered the month of oct 2007. Two radar types was searched for, one with high pulse repetition frequency (hprf) (causing peaks at an frequency interval of about 31Hz) and one radar with a lower pulse repetition frequency (lprf)(causing peaks in the frequency domain with a interval of about 214Hz).

Date	Hprf radar	Lprf radar	Other lines	Clean	Tot num files
2007-10-01	22	7	288	316	701
2007-10-02	22	7	288	319	703
2007-10-03	22	3	289	317	713
2007-10-04	22	6	274	326	701
2007-10-05	23	7	269	298	658
2007-10-06	29	10	293	319	699
2007-10-07	18	7	290	316	699
2007-10-08	15	10	276	293	674
2007-10-09	18	4	276	306	673
2007-10-10	26	6	294	310	704
Full Month	680	135	8282	9989	19616
Full Month (%)	3.4%	0.6%	42.2%	50.4%	100%

Table 6.1 indicates that about 50% of the occultations contains traces of at-least one more satellite but only 4% of the occultations contained radar signatures. The table also shows that the number of datasets with radar and other lines are fairly constant between consecutive days. It should be noted that one dataset can contain both types of radar and one other line and therefore contribute to all three types of interference.

Figure 6.1 indicates that most occultations with pulsed interference occur around eastern Asia and western North America. The figure shows only the location of the occultations and it gives no indication of how the antenna of the satellite was oriented. One interesting thing about the figure is the number of occultations with no interference very close to occultations with radar. This could be caused by differences in the field of view from the different antennas.

6.2 (O-B)/B Ratio

Using the developed method the O-B/B values from ROMSAF were divided into three groups: Clean, multiple signals and radar. No consideration was taken to quality indicators in the data-files, since the focus was to detect if there is any impact from transmitters on the quality and not on the retrieval process as such. Since only a few O-B/B curves had values at all heights and the O-B/B curves vary with altitude, the histograms were calculated individually for each height. The results from the histogram calculations were saved in a matrix that later was plotted in a altitude vs % error plot where the color shows the number of traces at each point, Figure 6.2

To see how the individual traces looks for the curves, a Figure 6.3 was generated where all O-B/B was plotted.

There are minor differences between the types of occultations, since the differences are so small it is not possible to say anything conclusive about if there is any impact on the accuracy when the raw sampling part of the occultation data contains traces of other satellites or radar.

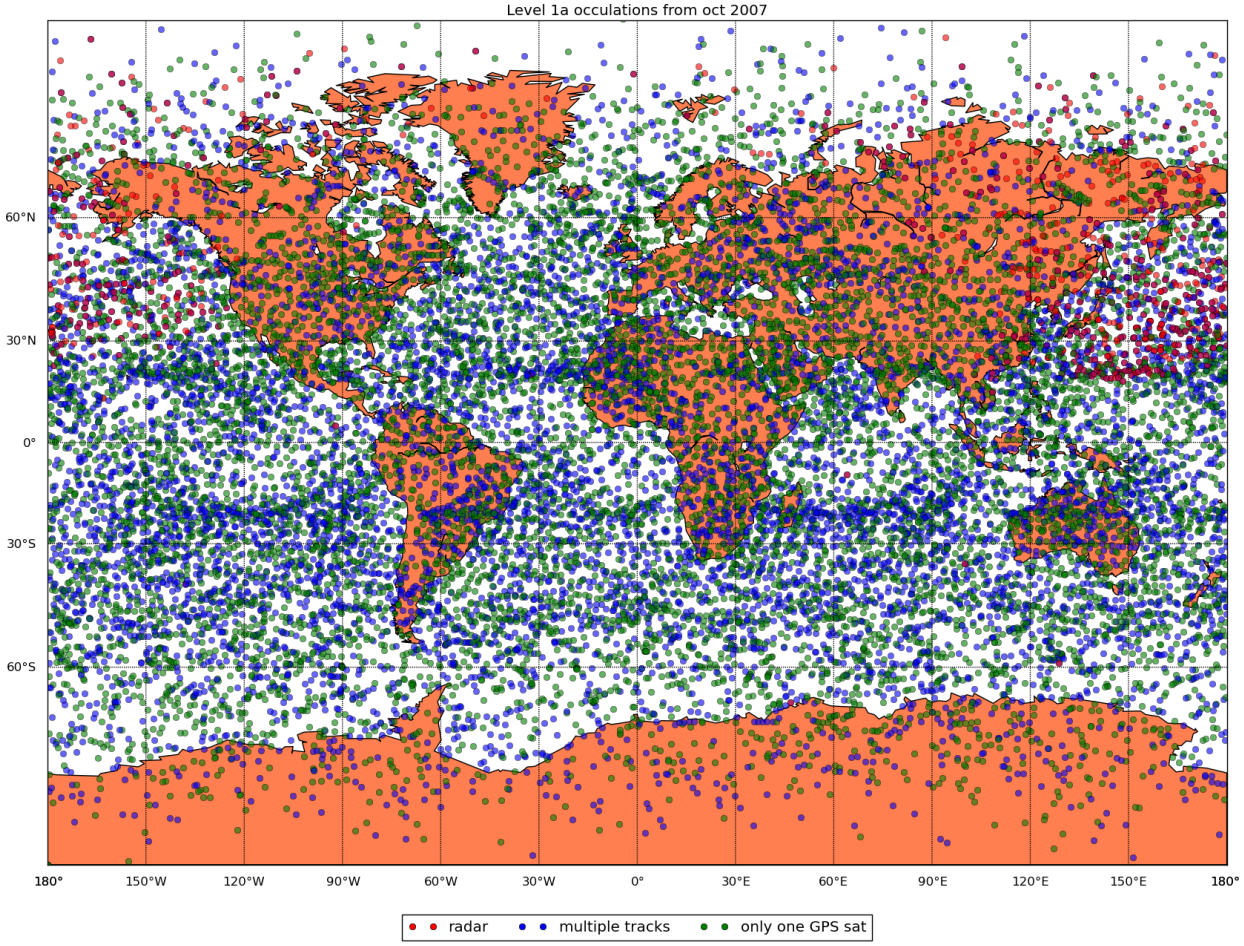

Figure 6.1: Global distribution of occultations during the month of Oct 2007

Both types of plots have the same layout, where the upper part shows a range of +-400% error and the lower parts shows +-40%.

The number O-B/B curves in each type was: 8398 clean profiles, 6619 profiles with multiple signals and 674 curves with pulsed interference.

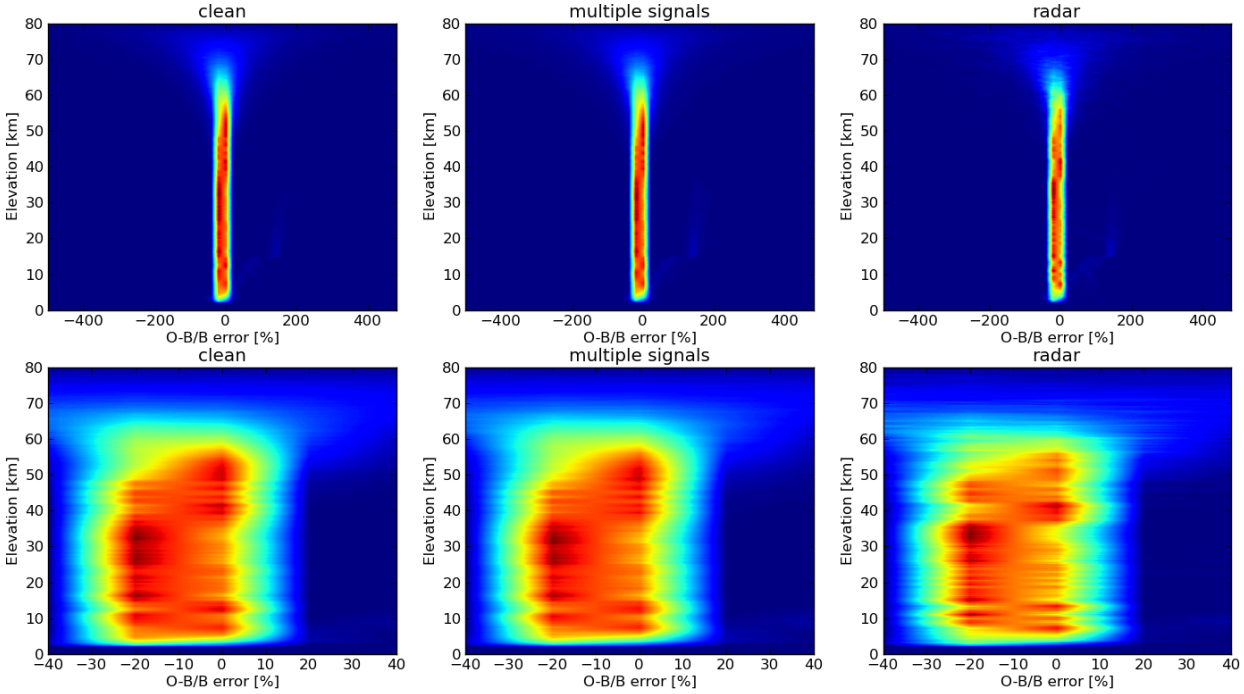

Figure 6.2: 'Histograms' over O-B/B ratios for clean, dataset with additional signal and dataset with radar

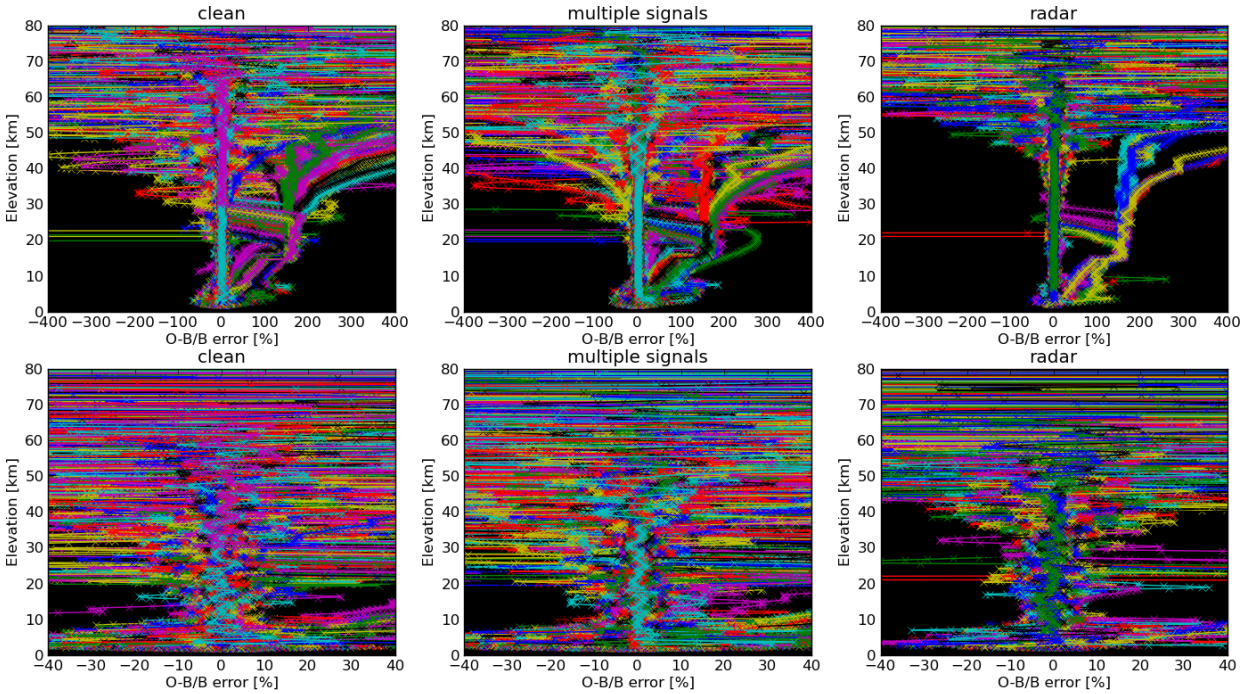

Figure 6.3: Indvidual O-B/B curves plotted for the month of Oct 2007

7. Summary and Outlook

One plot has been generated that shows the distribution of the level of background noise across the globe for a number of days in Oct 2007. The plot shows that the background noise is significantly higher on the northern hemisphere compared to the southern.

A method has been developed to automatically detect signals in the open-loop IQ data from the GRAS receiver. Analysis of L1a data from October 2007 showed that about 50% of the occultations contain signals from one or more sources than the tracked GPS satellite. Using the method a global plot was generated that shows where occultations with pulsed interference are recorded, as well as where the open loop data contains traces of other satellites as well as only the tracked satellite. The plot showed that the occultations with radar signatures are most common in the northern pacific whereas occultations with other signals or no additional signals are evenly spread around the globe. There does not seem to be any significant difference in the O-B/B results between datasets with a clean GPS signal, radar or other signals, although more research is needed to verify this.

The data analyzed shows only how the data looked during one month in 2007. By using more data it would be possible to do a more detailed analysis of the correlation between the different types of additional signals and the O-B/B ratio.

One example of where more data would improve the results is the O-B/B histograms. By using more data it would be possible to remove any RO that is "too bad" e.g. suffered from loss of L2 tracking. But also do statistics of how often the receiver looses L2 tracking when pulsed interference is present vs when the received signal is "clean". It seems as the number of additional signal does not impact the O-B/B but is this true for all cases?

There are a number of GNSS jamming exercise around the world every year, if and how these exercises have caused any impact on the RO measurement is yet to be determined. One problem with the GNSS jamming exercises are that the jamming signal in most cases are unavailable, but the approximate location and maximum jammed area is publicly available for air and maritime safety reasons.

A totally different approach, that have not been tested in the work would be to look at the worst (O-B)/B, say over x % at a certain altitude. Then determine if they share any common signal features (either in received signal power, location or raw sampling IQ data).

In figure 4.1 the analog gain applied to the received signal is plotted vs satellite position. One obvious question is what would the plot look like if the antenna ground pattern was taken into consideration? Also is the plot stable over the year or does it vary? (more fans in the summer for the A/C vs more "clean" electrical loads during the winter).